Protein tyrosine phosphatases ε and α perform nonredundant roles in osteoclasts

Eynat Finkelshtein[a], Sutada Lotinun[b], Einat Levy-Apter[a], Esther Arman[a], Jeroen den Hertog[c,d], Roland Baron[b], and Ari Elson[a]

[a]Department of Molecular Genetics, Weizmann Institute of Science, Rehovot 76100, Israel; [b]Department of Oral Medicine, Infection and Immunity, Harvard School of Dental Medicine, Boston, MA 02115; [c]Hubrecht Institute-Koninklijke Nederlandse Akademie van Wetenschappen and University Medical Center Utrecht, 3584 CX Utrecht, Netherlands; [d]Institute of Biology Leiden, Leiden University, 2333 BE Leiden, Netherlands

ABSTRACT **Female mice lacking protein tyrosine phosphatase ε (PTP ε) are mildly osteopetrotic. Osteoclasts from these mice resorb bone matrix poorly, and the structure, stability, and cellular organization of their podosomal adhesion structures are abnormal. Here we compare the role of PTP ε with that of the closely related PTP α in osteoclasts. We show that bone mass and bone production and resorption, as well as production, structure, function, and podosome organization of osteoclasts, are unchanged in mice lacking PTP α. The varying effects of either PTP on podosome organization in osteoclasts are caused by their distinct N-termini. Osteoclasts express the receptor-type PTP α (RPTPa), which is absent from podosomes, and the nonreceptor form of PTP ε (cyt-PTPe), which is present in these structures. The presence of the unique 12 N-terminal residues of cyt-PTPe is essential for podosome regulation; attaching this sequence to the catalytic domains of PTP α enables them to function in osteoclasts. Serine 2 within this sequence regulates cyt-PTPe activity and its effects on podosomes. We conclude that PTPs α and ε play distinct roles in osteoclasts and that the N-terminus of cyt-PTPe, in particular serine 2, is critical for its function in these cells.**

Monitoring Editor
Jonathan Chernoff
Fox Chase Cancer Center

Received: Mar 4, 2014
Revised: Mar 28, 2014
Accepted: Mar 28, 2014

INTRODUCTION

The mass of bone and its physical properties are regulated by the opposing activities of osteoblasts, which synthesize bone matrix, and osteoclasts, which degrade it. Osteoclasts are large, multinucleated cells that are formed by fusion of precursor cells from the hematopoietic monocyte-macrophage lineage in response to molecular signals, which include macrophage colony stimulating factor (M-CSF; CSF-1) and receptor activator of nuclear factor κB ligand (RANKL; Boyle *et al.*, 2003; Bruzzaniti and Baron, 2006; Teitelbaum, 2007). Osteoclasts (OCLs) adhere to bone, and from their ventral membrane they secrete acid and proteolytic enzymes onto the bone surface that degrade the organic and mineral components of the matrix (Bruzzaniti and Baron, 2006). OCLs adhere to matrix by use of podosomes—specialized adhesion structures that are centered on an actin-rich core. Integrins and associated molecules that surround the podosomal core transduce the signal generated by physical contact with matrix to the core, resulting in changes in its subcellular organization and stability (Destaing *et al.*, 2003, 2008; Luxenburg *et al.*, 2006b). The organization of podosomes in OCLs is typical of the activation state of the cell. Active osteoclasts (fully polarized cells, referring to the functional difference that develops in mature OCLs between their dorsal and ventral sides) that are grown on nondegradable surface are characterized by individually discernible podosomes that are arranged as a large array or belt at the cell periphery. In less-active or inactive (nonpolarized) cells, podosomes are organized in discrete rings, in smaller, less-developed clusters, or are spread at random throughout the cell.

Tyrosine phosphorylation of proteins plays central roles in the production of OCLs and in regulating their function. Phosphorylation is critical for signaling processes mediated by RANKL and M-CSF, whose receptor is the tyrosine kinase c-Fms (Ross, 2006; Wada *et al.*, 2006). Moreover, absence of the Src tyrosine kinase reduces

This article was published online ahead of print in MBoC in Press (http://www.molbiolcell.org/cgi/doi/10.1091/mbc.E14-03-0788) on April 2, 2014.

Address correspondence to: Ari Elson (ari.elson@weizmann.ac.il).

Abbreviations used: AKO, PTPa-deficient; cyt-PTPe, nonreceptor isoform of PTPe; DKO, deficient for both PTPs α and ε; EKO, PTPe-deficient; M-CSF, macrophage colony stimulating factor; OCL, osteoclast; PTP, protein tyrosine phosphatase; PTPa, PTP α; PTPe, PTP ε; RANKL, receptor activator of nuclear factor κB ligand; RPTPa, receptor isoform of PTPa; WT, wild type.

the ability of OCLs to resorb bone and organize their podosomal adhesion structures properly (Soriano *et al.*, 1991; Luxenburg *et al.*, 2006b; Miyazaki *et al.*, 2006; Destaing *et al.*, 2008). The kinase Pyk2, which functions in close collaboration with Src, also plays important roles in OCLs (Gil-Henn *et al.*, 2007). Physical contact of these cells with matrix activates integrin signaling and increases podosomal protein phosphorylation significantly (Luxenburg *et al.*, 2006a), further supporting the link between OCL adhesion, podosome function, and protein tyrosine phosphorylation. The central roles of tyrosine kinases in regulating OCLs indicate that tyrosine phosphatases, which counter kinase activity, also play critical roles in these processes. Among these, the nonreceptor-type PTP SHP1 inhibits OCL formation and function in vivo (Aoki *et al.*, 1999; Umeda *et al.*, 1999), whereas its close structural relative SHP2 performs opposite roles (Bauler *et al.*, 2011). The receptor-type PTP CD45 inhibits OCL function, leading to reduced OCL activity and increased bone mass in CD45-deficient mice (Shivtiel *et al.*, 2008). Loss of the dual-specificity phosphatase MKP1 in mice reduces the amount of OCLs but appears to render them more active (Carlson *et al.*, 2009; Sartori *et al.*, 2009). Studies in cell culture systems established the nonreceptor-type PTP-PEST as a positive regulator of OCL differentiation and adhesion, most likely through its role in dephosphorylating and activating Src and Pyk2 (Chellaiah *et al.*, 2007; Chellaiah and Schaller, 2009; Eleniste *et al.*, 2012). Similar findings were obtained in culture regarding the receptor-type PTPRO (PTP-oc; Amoui *et al.*, 2007; Yang *et al.*, 2007; Sheng *et al.*, 2009).

Protein tyrosine phosphatase ε (PTPe) is another positive regulator of OCL function. Two major protein forms of PTPe are known: the receptor type (RPTPe), which is an integral membrane protein, and the nonreceptor type (cyt-PTPe), which is predominantly cytosolic but can also be found in association with the cell membrane and in the nucleus. Both proteins are produced from the single *Ptpre* gene by use of alternative promoters (Krueger *et al.*, 1990; Elson and Leder, 1995a,b; Nakamura *et al.*, 1996; Tanuma *et al.*, 1999). RPTPe and cyt-PTPe are identical throughout their sequence, with the exception of their N-termini, where the transmembranal and extracellular domains of RPTPe are replaced in cyt-PTPe by a short sequence of 12 hydrophilic amino acids (Elson and Leder, 1995a). Two additional proteins are produced from the *Ptpre* gene: p67 PTPe, which is produced by initiation of translation at an internal ATG codon present in mRNAs for RPTPe and cyt-PTPe; and p65 PTPe, which is produced by proteolytic cleavage of RPTPe, cyt-PTPe, or p67 PTPe (Gil-Henn *et al.*, 2000, 2001). cyt-PTPe is expressed strongly in OCLs but not in osteoblasts; RPTPe is not expressed significantly in either cell type (Chiusaroli *et al.*, 2004). Young female homozygous PTPe-deficient mice (EKO mice; Peretz *et al.*, 2000), which lack all known forms of PTPe protein, exhibit increased trabecular bone mass, caused primarily by reduced OCL-mediated bone resorption. Accordingly, collagen telopeptide concentrations in serum of EKO mice are reduced, and OCL-like cells produced in vitro from bone marrow of EKO mice resorb mineralized matrix less well (Chiusaroli *et al.*, 2004). Recruitment of hematopoietic precursor cells from the bone marrow to the circulation, which depends on OCL function, is also reduced in female EKO mice (Kollet *et al.*, 2006). Loss of PTPe disrupts the structure, cellular organization, and stability of podosomes in OCLs and is consistent with reduced function of these cells (Chiusaroli *et al.*, 2004). After activation of integrin molecules, cyt-PTPe is phosphorylated at its C-terminal Y638 by partially activated Src; cyt-PTPe then dephosphorylates Src at Y527, thus fully activating the kinase and promoting OCL adhesion and activity (Granot-Attas *et al.*, 2009). Loss of cyt-PTPe disrupts podosomal structure and function at least in part due to reduced Src activation downstream of integrins (Chiusaroli *et al.*, 2004; Granot-Attas *et al.*, 2009).

The receptor-type PTP α (RPTPa) is closely related to RPTPe. Both PTPs are the only known members of the type IV subfamily of receptor-type PTPs, both possess short and heavily glycosylated extracellular domains, and the amino acid sequences of their catalytic domains and adjacent sequences are 72% identical. RPTPa is a ubiquitous protein that has been linked to, among other functions, cytoskeletal reorganization and cell migration (Zeng *et al.*, 2003; Chen *et al.*, 2006) and promotion of neural cell adhesion molecule–dependent neurite outgrowth (Bodrikov *et al.*, 2005). In several cases, RPTPa functions by dephosphorylating and activating Src or one of its related kinases (Zheng *et al.*, 1992; den Hertog *et al.*, 1993; Ponniah *et al.*, 1999; Su *et al.*, 1999), a property shared by PTPe (Berman-Golan and Elson, 2007; Granot-Attas *et al.*, 2009). A shorter form of RPTPa, p66 PTPa, is produced by proteolytic cleavage of RPTPa and is thus analogous to p65 PTPe (Gil-Henn *et al.*, 2001). No form of PTP α that is similar to cyt-PTPe is known. In this study we show that RPTPa does not play a unique role in OCLs. Building on this result, we analyze the contributions of various domains of RPTPa and cyt-PTPe, the form of PTPe that is present in OCLs, to the ability of either PTP to function in these cells. We find that the 12 N-terminal amino acid residues of cyt-PTPe, which are unique to this form of PTPe, and in particular serine 2 within this region, are critical for enabling cyt-PTPe to function in OCLs.

RESULTS

Mice lacking RPTPa exhibit normal bone structure

To examine whether RPTPa-deficient (AKO) mice exhibit abnormalities in bone structure, we first examined the expression of RPTPa in osteoclasts. In agreement with previous studies, protein blotting studies indicate that OCLs express both RPTPa and cyt-PTPe (Figure 1A; Chiusaroli *et al.*, 2004). As expected, RPTPa and cyt-PTPe were each absent from OCLs prepared from AKO or EKO mice, respectively (Figure 1A). Previous studies indicate that RPTPa, but not cyt-PTPe, is expressed in osteoblasts (Chiusaroli *et al.*, 2004).

Histomorphometric analysis of cancellous bone from tibiae of wild-type (WT) and AKO female mice did not reveal any abnormalities in AKO mice (Table 1). Partial bone volume, trabecular structure, bone formation rates, and the numbers and contact areas with bone of osteoblasts and OCLs were similar in WT and in AKO samples. Bone mineral density, measured by micro computerized tomography (micro-CT), was also similar in WT and AKO female mice (WT, 135.51 ± 13.48 mg/cc; AKO: 113.65 ± 9.04 mg/cc, $n = 6$ mice/genotype). In contrast, bone volume, trabecular number, and trabecular thickness were increased and trabecular separation was decreased in the EKO samples. Osteoblast parameters and most bone formation parameters were unaltered in EKO samples, as observed previously (Chiusaroli *et al.*, 2004); the apparently elevated mineralizing surface (MS)/bone surface (BS) values in EKO mice are not supported by the other bone synthesis and osteoblast parameters. A significant reduction in OCL numbers in EKO samples observed previously was not seen here, although a similar trend was observed. Histomorphometric analyses performed in parallel on tibiae from age- and strain-matched female mice lacking both phosphatases (DKO mice; Table 1) revealed increases in bone volume and trabecular number and thickness and decreased trabecular separation. In a manner distinct from the three other genotypes examined, DKO mice also exhibited significant increases in most bone-forming parameters, which may account for at least part of the observed increase in bone volume.

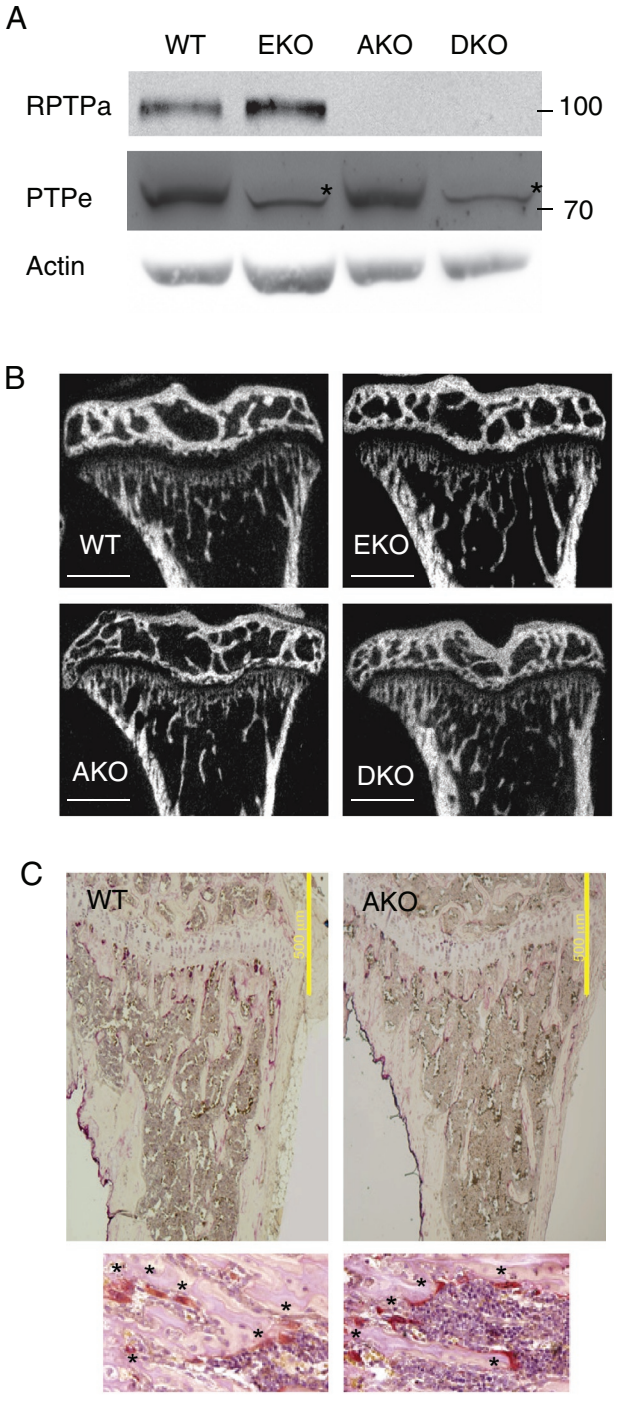

FIGURE 1: Bone structure of PTPa-deficient mice. (A) RPTPa is expressed in osteoclasts. Lysates prepared from osteoclasts differentiated in vitro from bone marrow precursors of WT, EKO, AKO, and DKO mice were probed with anti-PTPe/a antibodies. Molecular mass markers are in kilodaltons. Asterisk denotes a nonspecific background band in the PTPe blot. (B) Micro-CT images of tibiae of WT, EKO, AKO, and DKO female mice. Bar, 500 μm. (C) Top, section of tibiae from 7-wk-old WT and AKO male mice stained for TRAP. Bar, 500 μm. Bottom, higher magnification of bone section stained for TRAP (red, OCLs marked with asterisks) and counterstained with hematoxylin/eosin.

The appearance of AKO tibiae as analyzed by micro-CT was also normal (Figure 1B). Histological analysis of AKO tibiae revealed the presence of tartrate-resistant acid phosphatase (TRAP)–positive OCLs, and the fraction of bone surface that was in contact with OCLs in these preparations was similar in AKO and WT mice (Figure 1C and Table 1). In agreement, levels of collagen telopeptides in serum, an indication of OCL activity in vivo, were unchanged in AKO mice, indicating that bone resorption is unchanged in AKO mice (Table 2). We conclude that the absence of RPTPa does not disrupt normal bone structure or its formation or degradation in vivo. In these respects RPTPa differs considerably from cyt-PTPe, whose absence results in increased bone mass in vivo due to reduced OCL-mediated bone resorption (Chiusaroli *et al.*, 2004; Granot-Attas *et al.*, 2009; Table 1). RPTPa cannot compensate for loss of cyt-PTPe, indicating that their roles in this cell type are distinct.

RPTPa-deficient osteoclasts are produced and function normally in vitro

To examine the possible role of RPTPa in OCLs in greater detail, we isolated nucleated bone marrow cells from tibiae and femora of WT, AKO, EKO, and DKO mice. Cells were grown in culture in the presence of M-CSF and RANKL, which promote differentiation of precursor cells into OCL-like cells. Cells from mice of all four genotypes were produced similarly in vitro; the ability of AKO OCLs to resorb bone in vitro was similar to that of WT cells (Figure 2, A and B). Because the manner in which podosomes are arranged in OCLs correlates with their activity, we also scored the fraction of OCLs in culture in which podosomes were arranged as belts at the cell periphery, in small rings, or as clusters/at random (Figure 2C). OCL cultures prepared from WT and AKO mice contained similar fractions of cells in each of these three structural categories. In contrast, EKO OCLs exhibited a marked shift in podosomal organization: the fraction of OCLs containing a well-formed sealing zone–like structure was decreased significantly, whereas more cells displayed podosomes arranged at random (Figure 2D; Chiusaroli *et al.*, 2004; Granot-Attas *et al.*, 2009). Podosomal organization in DKO OCLs was similar to that in EKO OCLs (Figure 2D). We conclude that RPTPa does not perform a unique role in podosomal organization in OCLs in culture: its absence does not affect normal podosomal organization in WT OCLs, whereas the disruption observed in podosomal organization when PTP ε is absent is not affected by the presence or absence of RPTPa.

Phosphorylation of the C-terminal tyrosine of PTPs α and ε is often critical to allow these PTPs to fulfill their physiological roles (e.g., Zheng *et al.*, 2000; Berman-Golan and Elson, 2007; Sines *et al.*, 2007; Rousso-Noori *et al.*, 2011). In OCLs, cyt-PTPe is phosphorylated at Y638 after integrin-mediated contact with matrix, thus increasing the ability of cyt-PTPe to activate Src. In agreement, Src activity is reduced in EKO OCLs, and increasing Src activity can correct the abnormal stability of podosomes in EKO OCLs (Granot-Attas *et al.*, 2009). The C-terminal sequences of cyt-PTPe and RPTPa proteins are almost identical (Figure 3A), and phosphorylation of RPTPa at its C-terminal Y789 was shown to affect the physiological role of RPTPa in a number of nonbone systems. Examination of RPTPa in OCLs differentiated from primary bone marrow cells of WT mice indicated that this PTP is phosphorylated at Y789 in adherent OCLs. Phosphorylation of Y789 is not detected in OCLs held in suspension but is detected when these cells are allowed to reattach to a surface coated with fibronectin, a ligand of the αVβ3 integrin present in OCLs (Figure 3B). Physical contact of OCLs with matrix therefore induces C-terminal phosphorylation of RPTPa, much as it does for cyt-PTPe (Granot-Attas *et al.*, 2009). However, autophosphorylation of Src at Y416, an indicator of Src activity that is reduced in adherent EKO OCLs (Granot-Attas *et al.*, 2009), is unchanged in adherent AKO OCLs (Figure 3C), indicating that RPTPa is not

Parameter	WT (n = 7)	AKO (n = 7)	EKO (n = 7)	DKO (n = 8)
BV/TV (%)	3.44 ± 0.53	3.24 ± 1.01	9.61 ± 1.41*,+	11.49 ± 2.84*,+
Tb.Th (μm)	22.45 ± 1.85	22.62 ± 2.43	32.02 ± 1.26*,+	31.68 ± 2.54*,+
Tb.N (/mm)	1.51 ± 0.17	1.31 ± 0.22	2.94 ± 0.35*,+	3.31 ± 0.63*,+
Tb.Sp (μm)	700 ± 95	843 ± 102	341 ± 47*,+	365 ± 81*,+
MS/BS (%)	22.36 ± 2.42	22.45 ± 2.51	32.63 ± 3.79*,+	36.03 ± 1.32*,+
MAR (μm/d)	2.71 ± 0.28	2.83 ± 0.35	2.50 ± 0.19	3.14 ± 0.19
BFR/BS ($\mu m^3/\mu m^2$/yr)	215 ± 23	219 ± 23	287 ± 32	410 ± 20*,+,#
BFR/BV (%/yr)	2024 ± 303	1976 ± 184	1834 ± 244	2670 ± 181
Ob.S/BS (%)	15.50 ± 2.79	17.16 ± 2.14	13.07 ± 2.54	24.54 ± 3.63*,#
N.Ob/BS (/mm)	11.51 ± 2.43	14.66 ± 1.60	11.14 ± 2.62	21.53 ± 2.95*,#
OS/BS (%)	10.95 ± 2.61	15.82 ± 2.83	13.21 ± 2.47	16.91 ± 2.72
O.Th (μm)	3.88 ± 0.42	3.83 ± 0.42	4.64 ± 0.38	4.86 ± 0.38
Oc.S/BS (%)	11.36 ± 1.40	10.86 ± 2.08	7.39 ± 1.91	8.58 ± 2.04
N.Oc/BS (/mm)	5.39 ± 0.52	4.93 ± 1.11	3.42 ± 0.88	4.02 ± 0.95

Parameters are trabecular bone volume (BV/TV); trabecular thickness (Tb.Th); trabecular number (Tb.N); trabecular spacing (Tb.Sp); mineralizing surface (MS/BS); mineral apposition rate (MAR); bone formation rate per unit bone surface area (BFR/BS); bone formation rate per bone volume (BFR/BV); percentage bone surface in contact with osteoblasts (Ob.S/BS); osteoblast number per unit of bone surface length (N.Ob/BS); osteoid surface (OS/BS); osteoid thickness (O.Th); percentage bone surface in contact with osteoclasts (Oc.S/BS); and osteoclast number per unit bone surface length (N.Oc/BS). Similar values were obtained for BV/TV, Tb.SP, Tb.Th, and Tb.N in 7-wk-old WT and AKO female mice by micro-CT (unpublished data).
*$p < 0.05$ compared with WT.
+$p < 0.05$ compared with AKO.
#$p < 0.001$ compared with EKO.

TABLE 1: Histomorphometric analysis of the cancellous region of the tibial metaphysis of 7-wk-old female mice.

essential for activation of Src in these cells. Phosphorylation of Src at Y416 is reduced in DKO OCLs to levels observed in adherent EKO OCLs (Figure 3C), further indicating that RPTPa does not play a unique role in OCLs in this respect as well. pY416 Src, which is detected in adherent OCLs, is reduced significantly in OCLs held in suspension and is restored in an integrin-mediated manner when OCLs are allowed to readhere to a surface coated with fibronectin (Figure 3D). Despite their initial differences in pY416 Src levels (Figure 3C), OCLs from WT, EKO, AKO, and DKO mice were all capable of reattaching to fibronectin-coated surface and restoring initial levels of pY416 Src (Figure 3D). This indicates that cyt-PTPe is not the exclusive regulator of integrin-mediated activation of Src, which can occur to some extent in the absence of this phosphatase, possibly by other PTPs or directly by the β-integrin chain (Arias-Salgado *et al.*, 2003). In all, the role of RPTPa in production or function of OCLs in vivo or in vitro is either minimal or is redundant with the roles of other, non-PTP ε, PTPs.

	Serum CTX (ng/ml)
WT	108.1 ± 7.7
AKO	121.3 ± 10.8
EKO	72.9 ± 3.8*
DKO	95.1 ± 5.8

Shown are mean ± SE, n = 16–18 mice/genotype. *$p = 0.00004$ vs. WT by Student's t test.

TABLE 2: Collagen telopeptide concentrations in serum of 7-wk-old female mice.

Critical role for the N-terminus of cyt-PTPe in osteoclasts

The high degree of similarity between the catalytic domains of RPTPa and cyt-PTPe led us to examine the molecular basis for their nonredundant roles in OCLs. We note that in addition to each being the product of a distinct gene and displaying a slightly different sequence, the isoform of PTP ε that is expressed in OCLs is the nonreceptor, predominantly cytosolic cyt-PTPe, whereas RPTPa is a receptor-type integral membrane protein (Figure 4, A and B). To determine whether either of these distinctions affects the function of these PTPs in OCLs, we examined the abilities of various forms of PTPs α and ε to function in OCLs, using rescue of the podosomal disorganization observed in EKO OCLs as readout.

Stability and proper organization of podosomes in OCLs have been linked repeatedly with the ability of these cells to resorb matrix (e.g., Chiusaroli *et al.*, 2004; Miyazaki *et al.*, 2004; Gil-Henn *et al.*, 2007; Destaing *et al.*, 2008; Granot-Attas *et al.*, 2009). Podosomes of EKO OCLs are abnormally stable and disorganized, with relatively few EKO OCLs displaying a well-organized podosomal belt at their periphery. Expression of cyt-PTPe in EKO OCLs rescues their abnormal podosomal stability (Chiusaroli *et al.*, 2004; Granot-Attas *et al.*, 2009). To examine whether cyt-PTPe could also rescue podosomal organization in EKO OCLs, we infected these cells with adenoviruses expressing cyt-PTPe. OCLs in which podosomes were arranged as a podosomal belt at the cell periphery, in small rings, or in clusters (Figure 2C) were scored and compared with those seen in WT and in mock-infected EKO OCLs. As seen in Figure 4C, expression of WT cyt-PTPe in EKO OCLs rescued their abnormal podosome organization pattern and made it similar to that of WT OCLs, thus validating use of podosomal organization as a readout for the EKO OCL phenotype in this study.

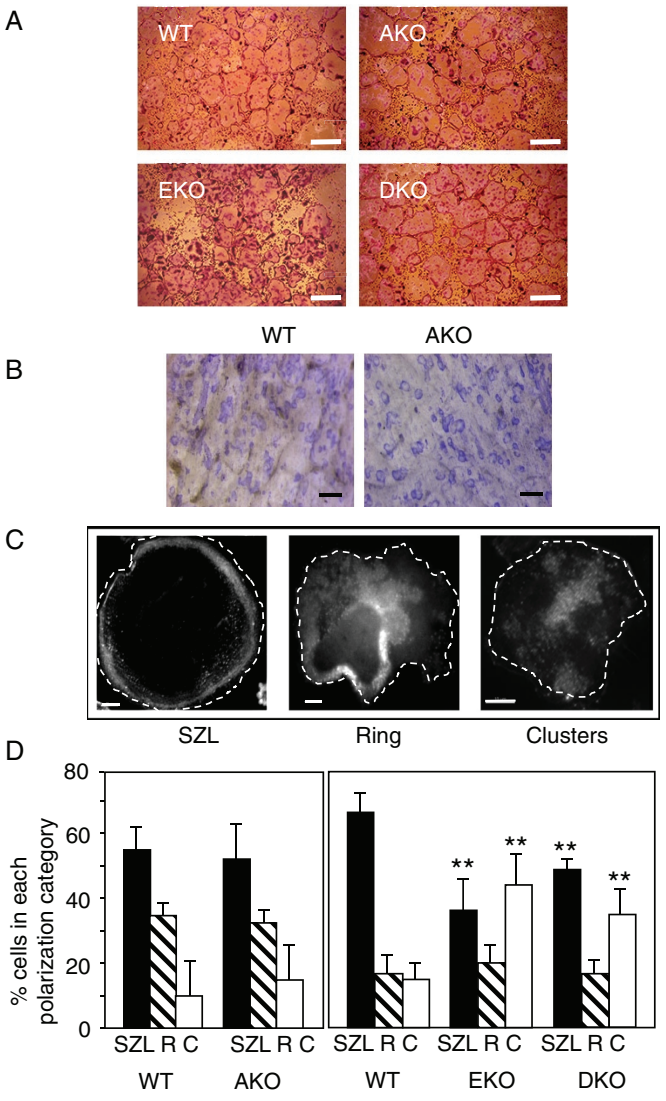

FIGURE 2: Properties of PTP α-deficient osteoclasts. (A) Bone marrow cells from WT, AKO, EKO, and DKO female mice were cultured with M-CSF and RANKL for 6 d and then stained for TRAP (red). Bar, 200 μm. (B) Bone marrow cells from WT and AKO female mice were seeded on fragments of bovine bone and grown for 8 d in the presence of M-CSF and RANKL. Cells were then removed and the bone fragments stained with Coomassie brilliant blue to highlight resorption pits. Bar, 400 μm. (C) WT OCLs prepared from 7-wk-old female mice were grown on glass coverslips, fixed, stained with phalloidin–Alexa 488, and examined by cell imaging. Shown are examples of the three podosomal arrangement types: sealing zone–like structure (SZL, large single belt at the cell periphery), rings (mixture of small rings and individual, scattered podosomes), and clusters (individual or grouped podosomes, no rings). Bar, 10 μm. Dashed line marks outer perimeter of the cell shown. (D) Percentages (mean ± SD) of OCLs of the four genotypes in which the actin-rich podosomal cores were arranged in SZL-like structures (SZL), rings (R), or clusters (C). $n = 317–638$ OCLs/genotype. $^{**}p < 0.05$ vs. WT by Student's t test.

To compare the effect of various forms of PTPs α and ε on podosomal organization in EKO OCLs, we constructed a series of adenoviral expression vectors for expressing proteins shown in Figure 4A. Each adenoviral vector was able direct expression of the relevant protein product (Supplemental Figure S1), and its effect on podosomal organization was scored. As seen in Figure 4D, the fraction of

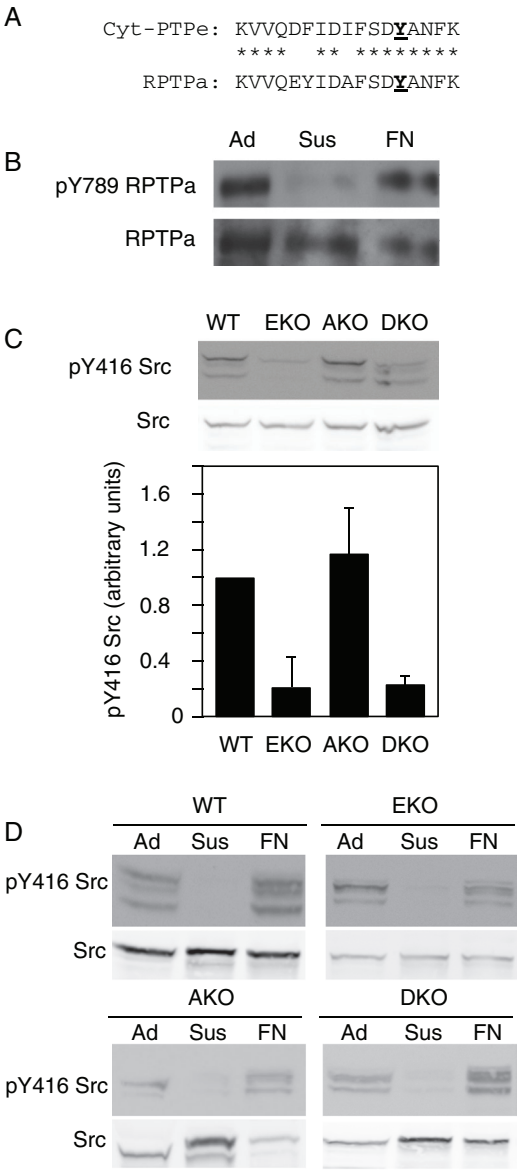

FIGURE 3: Phosphorylation of RPTPa and Src in OCLs. (A) C-terminal sequences of cyt-PTPe and RPTPa. The phosphorylatable tyrosine (Y789 in RPTPa, Y638 in cyt-PTPe) is highlighted. (B) Primary OCLs prepared from bone marrow of WT mice were grown on plastic plates (Ad), serum-starved, lifted, maintained in suspension for 30 min (Sus), and then seeded on plates coated with fibronectin (FN). Cells were lysed, and pY789 RPTPa was detected by protein blotting. (C) Phosphorylation of Src at its activating Y416 in adherent OCLs from WT, EKO, AKO, and DKO female mice. Top, representative protein blot. Bottom, bar diagram summarizing two to seven independent repeats per genotype (each compared with pY416 Src levels in WT OCLs processed in parallel; mean ± SE). (D) Src undergoes integrin-dependent phosphorylation in the absence of PTP α and/or ε. Adherent, suspended, and readherent OCLs from the four genotypes were analyzed for pY416 Src by protein blotting. Note that in all cases, Src is hypophosphorylated in suspended cells (Sus) and rephosphorylated when cells readhere for fibronectin-covered surface (FN). Intensity of pY416 Src phosphorylation varies among genotypes as in C; exposure of pY416 Src images was adjusted for each genotype to allow visualization of phosphorylation.

EKO OCLs that displayed a well-organized podosomal belt was significantly lower than in WT OCLs. Expressing in EKO OCLs either cyt-PTPe or the artificial protein cyt-PTPa, in which the 12 N-terminal

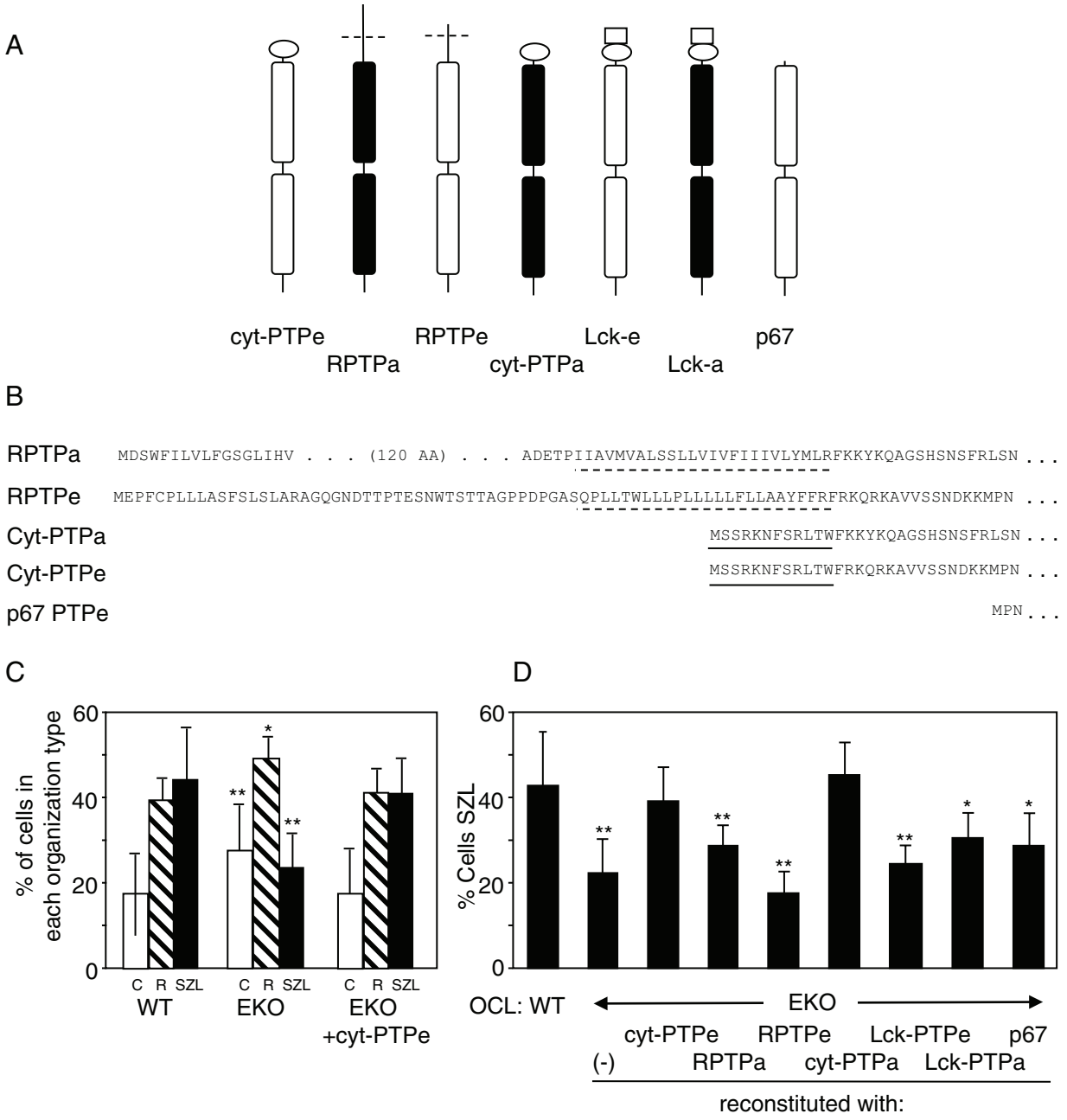

FIGURE 4: Nonreceptor forms of PTPs ε and α can rescue the podosomal organization phenotype of EKO osteoclasts. (A) Schematic representation of various constructs of PTP ε and PTP α used in this study. Dashed horizontal lines, cell membrane; oval, unique N-terminus from cyt-PTPe; small rectangle, Lck myristoylation motif; large vertical rectangles, PTP domains of PTP α (black) or PTP ε (white). (B) N-terminal sequences of RPTPa/e, cyt-PTPa/e, and p67 PTPe. Dashed underline marks membrane-spanning regions of RPTPe and RPTPa. Solid underline marks the 12 N-terminal residues of cyt-PTPe, which are unique to this isoform (and were included as the N-terminus of the artificial cyt-PTPa protein). (C) Expression of cyt-PTPe in OCLs from PTPe-deficient mice rescues their podosomal organization phenotype. Cultures of OCLs prepared from bone marrow of WT or EKO mice, some expressing exogenous cyt-PTPe as indicated, were examined as described in Figure 2D. $*p \leq 0.03$, $**p \leq 0.006$ vs. WT by Student's *t* test. $n = 199–918$ OCLs per genotype and treatment. (D) Rescue of the EKO OCL podosome organization phenotype by various PTP ε and PTP α molecules. WT and EKO OCLs prepared from 7-wk-old female mice infected with adenoviruses expressing the indicated constructs and then processed as in Figure 2D. Percentage of cells (mean ± SD) in which podosomes are arranged as a podosomal belt (SZL) for clarity of presentation. The complete distributions of SZL, R, and C cells in this experiment are shown in Supplemental Figure S2. $*p \leq 0.04$, $**p \leq 0.008$ vs. WT. $n = 199–918$ osteoclasts analyzed per treatment.

residues of cyt-PTPe replaced the membrane-spanning and extracellular domain of RPTPa (Figure 4B), increased the fraction of cells displaying well-organized podosomal belt structures to that found in WT OCLs. In contrast, RPTPe and RPTPa did not do so. We conclude that despite the sequence differences that exist between them, the catalytic domains of both PTPs can function in OCLs to

ensure proper podosomal organization. We also conclude that the distinction between the N-terminal sequences of both PTPs affects their ability to function in OCLs.

Lck-PTPe and Lck-PTPa, forms of cyt-PTPe or cyt-PTPa whose N-termini include an Lck myristoylation motif, did not rescue the podosomal organization phenotype of EKO OCLs (Figure 4D). Lck-tagged PTPs localize to the cell membrane (e.g., Andersen *et al.*, 2001) but lack the membrane-spanning and extracellular regions of RPTPe/RPTPa. This result indicates that interaction with extracellular ligands, such as dimerization-induced inhibition of RPTPa (Jiang *et al.*, 1999, 2000), is not the cause of the inability of both molecules to rescue the EKO OCL podosomal phenotype. Finally, p67 PTPe, which lacks the 27 N-terminal amino acid residues of cyt-PTPe and is entirely cytosolic (Figure 4B; Gil-Henn *et al.*, 2000), did not rescue the podosomal organization phenotype of EKO OCLs (Figure 4D). In all, the only forms of PTPs α and ε that rescued podosomal organization in EKO OCLs were cyt-PTPe and cyt-PTPa. Both proteins include the 12 N-terminal amino acids of cyt-PTPe, which are absent from all other proteins examined in this study. We conclude therefore that these 12 residues are required to allow cyt-PTPe to support proper organization of podosomes in OCLs.

We showed previously that cyt-PTPe is found also in podosomes of OCLs (Granot-Attas *et al.*, 2009). To determine whether p67 PTPe and cyt-PTPa proteins can be associated with podosomes, we expressed both proteins in EKO OCLs, isolated podosome-enriched fractions from the cells, and examined whether either protein is present in them. In these experiments fractionations of actin and Src, which are found throughout the cell and in podosomes, and of tubulin, which is not found in podosomes, were followed as controls for the quality of the fractionation process. This study revealed that cyt-PTPe and cyt-PTPa, which possess the N-terminus of cyt-PTPe, and p67, which does not, are all present in podosome-rich fractions of OCLs (Figure 5). We conclude therefore that despite its role in ensuring proper podosomal organization in OCLs, the N-terminus of cyt-PTPe is not required for actual localization of cyt-PTPe in podosomes. Of note, similar fractionation experiments revealed that RPTPa was not present in OCL podosome–enriched fractions irrespective of whether endogenous or exogenous RPTPa was examined (Figures 5 and 6E). It is therefore possible that at least part of the functional differences between cyt-PTPe and RPTPa in OCLs arise also from the absence of RPTPa from podosomes.

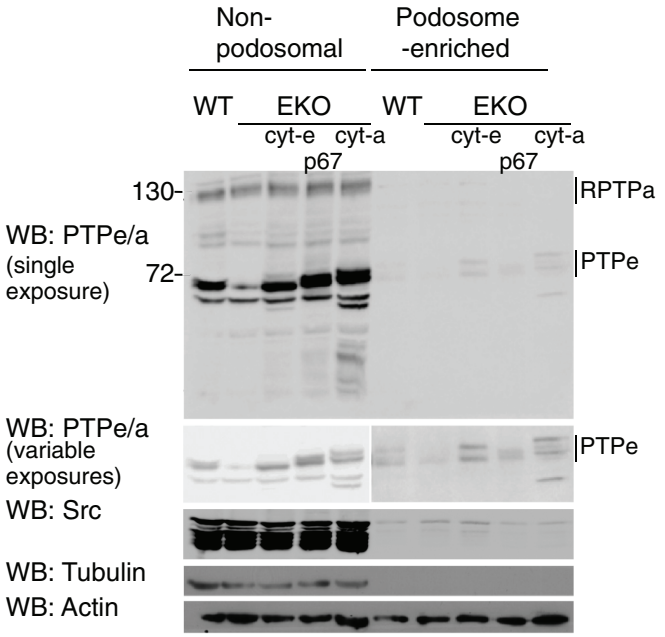

FIGURE 5: Effects of the N-terminus on podosomal localization of PTPs α and ε. (A) Cultures of WT and EKO osteoclasts, some expressing exogenous cyt-PTPe, p67 PTPe, or cyt-PTPa, were fractionated into podosome-enriched and nonpodosomal fractions. Shown are both fractions at the same exposure (top) and at different exposures (second from top; nonpodosomal is less exposed and podosome enriched is more exposed than in the top). Tubulin (fourth from top), which is not found in podosomes, and Src and actin (third from top, and bottom, respectively), which are found in both fractions, serve as controls for the fractionation process. The podosomal and nonpodosomal fractions were prepared in distinct buffers, which accounts for their slightly different electrophoretic migration patterns. Size markers are in kilodaltons.

Serine 2 affects cyt-PTPe activity and is required for cyt-PTPe to regulate podosome organization in OCLs

We next examined the 12 N-terminal residues of cyt-PTPe in further detail. As seen in Figure 6A, this sequence contains three positively charged residues (R4, K5, R9) and four potential phosphorylation sites (S2, S3, S8, T11). R4, K5, and R9 participate in a functional nuclear localization signal (Kraut *et al.*, 2002), making their involvement in podosomal regulation possibly less likely. We therefore turned our attention to serine 2, the first of the four serine/threonine residues. Expression of S2D cyt-PTPe, which mimics phosphorylation at this site, rescued the podosomal arrangement phenotype of EKO OCLs. In contrast, S2A cyt-PTPe, which mimics dephosphorylation at this site, did not do so. In fact, expression of this latter construct in EKO OCLs exacerbated podosomal disorganization, suggesting that it may function in a dominant-negative role (Figure 6B). We note that the catalytic activities of both S2A and S2D cyt-PTPe are higher than that of WT cyt-PTPe (Figure 6C). This result indicates that presence of serine 2 inhibits cyt-PTPe catalytic activity and suggests a regulatory role for this residue. However, the effect of serine 2 of cyt-PTPe on podosomal organization in OCLs is most likely not mediated by changes in cyt-PTPe activity, since S2A and S2D cyt-PTPe exert opposite effects on podosomal organization despite both being active and activating Src throughout the cell to similar extents in OCLs (Figure 6D).

Fractionation studies indicated that S2D cyt-PTPe and S2A cyt-PTPe are found in podosome-enriched fractions of OCLs to similar extents (Figure 6E), in agreement with our previous conclusion that the N-terminus of cyt-PTPe does not control podosomal localization of cyt-PTPe (Figure 5). The S2A and S2D mutations did not affect nuclear localization of cyt-PTPe (unpublished data), indicating that serine 2 does not interact functionally with the adjacent nuclear localization signal. These results strongly suggest that serine 2, possibly through its phosphorylation, is required for cyt-PTPe to regulate podosomal organization in OCLs.

DISCUSSION

Results presented here indicate that lack of RPTPa does not affect the mass or structure of trabecular bone. AKO mice also exhibit unaltered rates of bone synthesis and degradation, and their OCLs are produced, function, and signal normally. In parallel, we confirm that loss of the related cyt-PTPe disrupts the structure, stability, and organization of podosomes in OCLs and results in increased trabecular bone mass. Moreover, in all experiments performed in culture, OCLs from EKO mice performed identically to OCLs from DKO mice that lack both RPTPa and cyt-PTPe. Loss of RPTPa therefore did not affect the phenotypes induced by loss of cyt-PTPe. We

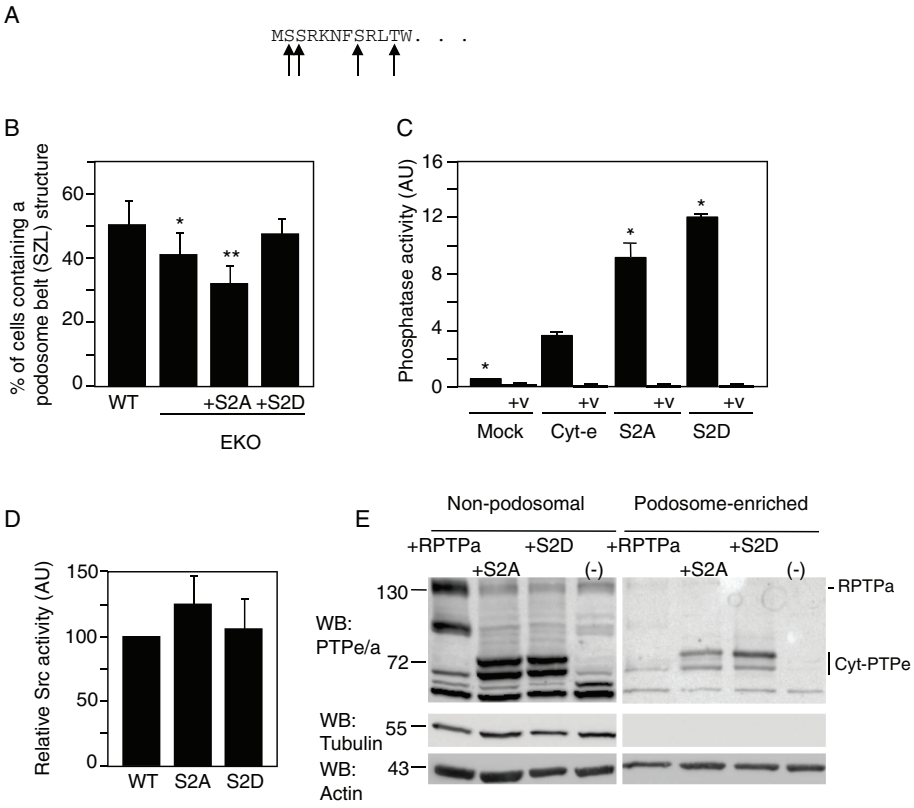

FIGURE 6: Serine 2 of cyt-PTPe regulates its function in osteoclasts. (A) Sequence of the 12 N-terminal residues of cyt-PTPe. Arrows mark S2, S3, S8, and T11. (B) S2A cyt-PTPe fails to rescue the EKO podosomal phenotype. Cultures of WT and EKO OCLs were infected with adenoviruses expressing S2A cyt-PTPe or S2D cyt-PTPe as indicated, and the organization of their podosomes was analyzed as in Figure 2D. Percentage of cells (mean ± SD) in which podosomes are arranged as a belt at the cell periphery. *$p = 0.02$, **$p = 0.0006$ vs. WT. $n = 370–709$ osteoclasts analyzed per genotype and treatment. (C) Serine 2 inhibits cyt-PTPe activity. A total of 293 cells expressing empty vector (mock) or cyt-PTPe proteins as indicated were lysed, and total phosphatase activity toward PNPP in the lysates was measured with or without presence of PTP inhibitor (0.5 mM sodium pervanadate; +v). Values represent mean ± SE; *$p < 0.03$ by Student's t test vs. cyt-PTPe. This experiment is representative of four to eight separate experiments. In all, fold increases in activities of S2A and S2D cyt-PTPe relative to WT cyt-PTPe were 1.53 ± 0.23 and 1.76 ± 0.37, respectively. (D) Src kinase activity is similar in EKO OCLs expressing WT, S2A or S2D cyt-PTPe (mean ± SE of five experiments). Activity in EKO OCLs devoid of PTP ε (unpublished data) was 0.67 ± 0.11 of cells expressing WT cyt-PTPe. (E) OCLs prepared from female EKO mice were infected with adenoviral vectors expressing S2A cyt-PTPe, S2D cyt-PTPe, or RPTPa as indicated. (–), mock-infected cells. Cells were fractionated and analyzed as described in Figure 5. Size markers are in kilodaltons.

conclude that loss of cyt-PTPe in OCLs cannot be compensated for by RPTPa. Our studies do not rule out the unlikely possibility that RPTPa is functionally redundant with another, more distantly related PTP rather than with its close relative, cyt-PTPe.

In contrast to DKO OCLs in culture, whose properties are similar to those of EKO OCLs, DKO mice exhibit increases in several parameters of bone production, whereas EKO and AKO mice do not (Table 1). Because cyt-PTPe is not expressed in osteoblasts (Chiusaroli *et al.*, 2004), inactivation of its gene would not be expected to affect these cells directly, leaving open the possibility that loss of PTP ε affects osteoblasts in an indirect manner. Hypothalamic leptin signaling can affect osteoblasts via the sympathetic nervous system and other pathways (Takeda *et al.*, 2002; Elefteriou *et al.*, 2005; Yadav *et al.*, 2009). We showed previously that PTP ε down-regulates leptin receptor signaling in the hypothalamus, leading to increased leptin sensitivity and resistance to diet-induced obesity in female EKO mice (Rousso-Noori *et al.*, 2011). It is then possible that loss of both PTPs α and ε affects hypothalamic leptin signaling to an extent that affects osteoblast function indirectly.

Data presented here then differentiate RPTPa from the closely related cyt-PTPe, which supports OCL-mediated bone resorption in part by activating Src downstream of integrin receptors (Granot-Attas *et al.*, 2009). Although both PTPs are closely related and perform several of their physiological functions by dephosphorylating and activating Src, loss of cyt-PTPe, but not RPTPa, reduces Src activity in cultured OCLs (Figure 3C); this suggests that these PTPs differ in their ability to activate Src in OCLs. Because proper Src activity is essential for OCL function, this may explain in part the functional differences between both PTPs. This functional distinction most likely arises from a more basic difference between the isoforms of these PTPs that are expressed in OCLs—the receptor-type RPTPa versus the nonreceptor-type cyt-PTPe. RPTPa and its receptor-type PTP ε counterpart RPTPe cannot rescue the podosomal organization phenotype of EKO OCLs. In contrast, cyt-PTPe and the similarly structured artificial protein cyt-PTPa do rescue this phenotype; this indicates that despite some sequence differences between both PTPs, the catalytic domains of PTP α can function in OCLs when presented in the proper structural context.

Functional differences in the phenotypes of osteoclasts lacking one of two such closely related PTPs provide an opportunity to identify domains within cyt-PTPe that are essential for its function in this cell type. The main structural feature that sets apart RPTPa from cyt-PTPe is the presence of transmembranal and extracellular domains in RPTPa, which are replaced by a unique sequence of 12 amino acids in cyt-PTPe (Figure 4). The inability of RPTPa and the related RPTPe to rescue podosomal organization in EKO OCLs might be caused by the absence of the 12 N-terminal residues of cyt-PTPe from both PTPs or by a particular function that is fulfilled actively by the transmembranal and extracellular domains of either PTP. The latter active model is not likely, since the sequences of the extracellular domains of RPTPe and RPTPa differ significantly from each other and from the N-termini of Lck-PTPa, Lck-PTPe, and p67, which also cannot regulate podosomal organization. The active model would rely on the unlikely assumption that the widely divergent N-termini of these five molecules share the ability to actively prevent rescue of the podosomal organization phenotype of EKO OCLs. These results also argue against the possibility that RPTPe and RPTPa are inhibited from functioning in OCLs by binding of an extracellular ligand(s). The alternative model, by which presence of the 12 N-terminal amino acids of cyt-PTPe is required for affecting podosomal organization in OCLs, is strengthened significantly by the finding that the S2A mutation in this sequence

abrogates its ability to do so. The latter results highlight the importance of serine 2 in regulating cyt-PTPe in OCLs and raise the possibility that cyt-PTPe function in OCLs is regulated by phosphorylation at this residue.

The mechanism by which serine 2 affects cyt-PTPe function in osteoclasts is not clear. The 12 N-terminal residues of cyt-PTPe do not control physical access of cyt-PTPe to podosomes, since cyt-PTPe and its mutants S2A and S2D, as well as p67, which lacks this sequence, are all detected in podosome-enriched fractions of OCLs. Although serine 2 down-regulates the catalytic activity of cyt-PTPe, activity alone does not explain the ability of cyt-PTPe to regulate podosomal organization, since S2A and S2D cyt-PTPe, which affect podosomal organization in opposite ways, are similarly active. It is possible that the N-terminus of cyt-PTPe allows it to engage in protein–protein interactions or regulates protein stability in a way that is essential for its function in osteoclasts; further studies are needed to address this issue.

MATERIALS AND METHODS

Antibodies

Polyclonal antibodies used included anti-PTPe (Elson and Leder, 1995b), which cross-reacts with RPTPa; anti–phospho-PTPe, which reacts specifically with PTP ε phosphorylated at its C-terminal tyrosine residue (Y638 in cyt-PTPe = Y695 in RPTPe; Berman-Golan and Elson, 2007) and cross-reacts with RPTPa phosphorylated on its C-terminal Y789; and anti-pY416 Src (Cell Signaling Technology, Danvers, MA). Monoclonal antibodies used included anti–v-Src (clone 327; Calbiochem, San Diego, CA), anti–α-tubulin (clone DM1A; Sigma-Aldrich, St. Louis, MO), and anti-actin (clone AC-40; Sigma-Aldrich). Horseradish peroxidase (HRP)–conjugated secondary antibodies for protein blotting were from Jackson ImmunoResearch Laboratories (West Grove, PA). Enhanced chemiluminescence reagents were from Biological Industries (Beit Haemek, Israel).

Mice

Gene-targeted mice lacking PTP ε (Peretz *et al*., 2000) or RPTPa (Bodrikov *et al*., 2005), as well as DKO mice lacking both PTPs and WT controls, were used in a mixed 50% 129 SvEv, 50% C57Black/6 genetic background. In some studies EKO and WT mice were in the pure 129 SvEv background. All mice were handled in accordance with Israeli law and Weizmann Institute regulations, and studies were approved by the Weizmann Institute's Animal Ethics Committee.

Micro-CT and bone histomorphometry

Micro-CT was performed on a volume of 1.8 mm^3 of cancellous bone starting 0.3 mm distal to the proximal tibial growth plate, using an eXplore Locus SP system (GE Healthcare, London, Canada). Histomorphometric measurements were performed on 5-μm sagittal sections of tibiae embedded in methyl methacrylate resin as described (Aoki *et al*., 1999). Histomorphometric parameters were measured in a 1.84-mm^2 area of secondary spongiosa starting 0.3 mm from the proximal growth plate, using the Osteomeasure analysis system (Osteometrics, Atlanta, GA). Data were analyzed for statistical significance by Student's *t* test.

Osteoclast culture

Bone marrow from femora and tibiae of 6- to 8-wk-old mice was depleted of erythrocytes by hypotonic lysis and cultured in complete OCL medium (α-MEM [Sigma-Aldrich] containing 10% fetal calf serum [Invitrogen-Life Technologies, Carlsbad, CA], 2 mM glutamine, 50 U/ml penicillin, and 50 g/ml streptomycin and supplemented with 20 ng/ml M-CSF [Peprotech, Rocky Hill, NJ] and 20 ng/ml RANKL [R&D Systems, Minneapolis, MN]). Cell were plated at 5×10^6 or 1×10^6 cells per well of a six- or 24-well plate, respectively, and incubated at 37°C in 5% CO2 for 5 d with daily changes of medium. Cells were fixed and stained for TRAP activity using a commercial kit (Sigma-Aldrich).

Pit resorption assay

Bone marrow cells were cultured on bovine cortical bone slices for 7–8 d with M-CSF and RANKL. Cells were removed from bone by treatment with 0.25M NH_4OH. The slices were washed in distilled water, incubated in a saturated alum ($KAl(SO_4)_2$) solution, washed in distilled water, and stained with Coomassie brilliant blue (0.2% in a solution of 40%H_2O/60% methanol).

Collagen telopeptide assay

Serum was prepared from blood collected by retro-orbital bleeding from 7-wk-old female mice that had been fasted overnight. Concentrations of C-telopeptide degradation products of type I collagen were determined using the Ratlaps ELISA system (Immuneodiagnostics Systems, Scottsdale, AZ) according to the manufacturer's instructions.

Replating experiments

Primary bone marrow preosteoclasts were starved on their fourth day of differentiation for 4 h in OCL medium containing 1% serum and no cytokines. Cells were detached by a short treatment with 10 mM EDTA, suspended in DMEM containing 20 mM HEPES and 1 mg/ml bovine serum albumin, and incubated at 37°C for 1 h with gentle rotation. Cells were replated on plates precoated with 20 μg/ml fibronectin (Sigma-Aldrich) and analyzed 30 min later.

Adenoviral infection of OCLs

Bone marrow from mice was cultured in OCL medium as described. Two days after seeding, medium was replaced with complete OCL medium containing adenoviruses. After overnight incubation the medium was changed and the cells were fed daily with fresh OCL medium (containing cytokines). Adenoviruses were produced with AdEasy XL adenoviral vector system (Stratagene, Agilent Technologies, Santa Clara, CA).

Fluorescence microscopy

BM cells were seeded on glass coverslips (Menzel-Glaser, Braunschweig, Germany). On day 2 of differentiation, cells were infected with adenoviruses; after 4 d of differentiation, OCLs were fixed in 3% paraformaldehyde (PFA; Merck, Darmstadt, Germany) in phosphate-buffered saline (PBS) for 20 min and then for an additional 2 min in warm 3% PFA containing 0.5% Triton X-100 (Sigma-Aldrich). After staining with phalloidin conjugated to Alexa 488, cells were mounted with Fluoromount-G solution (Southern Biotech, Birmingham, AL). Images were collected on a deconvolution DeltaVision microscope system equipped with Resolve3D software (Applied Precision, Issaquah, WA). Cells were analyzed visually and scored as displaying a complete podosomal belt structure (fully polarized, FP), partial podosomal belt and rings (partly polarized, PP), or podosomes arranged small clusters or at random (nonpolarized, NP). Analyses were performed in a manner blinded to the genotypes of the cells.

Differential cell lysis

Primary OCLs were cultured in six-well plates and in some samples infected with adenoviruses as described. Cells were lysed in

200 µl/well lysis buffer (20 mM Tris-HCl, pH 7.4, 5 mM EDTA, 1% Triton, and 1 mM sodium vanadate with protease inhibitors [1 mM 4-(2-aminoethyl) benzenesulfonyl fluoride, 40 µM bestatin, 15 µM E-64, 20 µM leupeptin, 15 µM pepstatin; Sigma-Aldrich]) on ice for 10 min with gentle shaking. Cell bodies and cytoplasm were removed and saved. The remaining adherent podosomal structures were washed gently three times with 200 µl of lysis buffer. Lysis buffer was completely removed, and the remaining cell structures were solubilized in 100 µl/well of 20 mM Tris-HCl, pH 7.4, 5 mM EDTA, 0.1% SDS, and 1% sodium deoxycholate with protease inhibitors.

Protein blotting

Cells were washed with ice-cold PBS and lysed in NP40 buffer (50 mM Tris-Cl, pH 8; 150 mM NaCl; 1% NP-40) and protease inhibitors. Sodium pervanadate, 0.5 mM, was included when tyrosine phosphorylation of proteins was evaluated. A 25-µg amount of total lysates was subjected to 7% SDS–PAGE and transferred onto a nitrocellulose membrane (Protran; Whatman GE Healthcare, Maidstone, United Kingdom). The filters were blocked in 5% milk/PBS/Tween for 1 h and incubated with primary antibody at 4°C overnight, followed by probing with secondary antibodies coupled to HRP.

Activity assays

For the PTP ε activity assay, the various forms of PTP ε were expressed at similar levels in 293 cells. At 48 h after transfection, cells were lysed in NP-40 buffer supplemented with protease inhibitors. Total phosphatase activity in lysates was assayed in duplicate at 30°C in 96-well plates in reactions containing 100 µl of cell lysate (25 µg of total protein) and 200 µl of assay buffer (50 mM 2-(*N*-morpholino)ethanesulfonic acid, pH 7.0, 0.5 mM dithiothreitol, 0.5 mg/ml bovine serum albumin, and 10 mM *p*-nitrophenyl phosphate). Each sample was assayed with or without addition of 0.5 mM PTP inhibitor sodium pervanadate. Activity was measured by following the increase in absorbance at 405 nm for 45 min, during which absorbance was linear with time. Net activity of each form of PTP ε was normalized to its expression level as determined by protein blotting. Src activity was determined by measuring phosphorylation of enolase by Src immunoprecipitated from the cells analyzed, as described in Gil-Henn and Elson (2003).

ACKNOWLEDGMENTS

We are grateful to Eli Zelzer and Amnon Sharir, Meir Barak, and Chagai Rot for assistance in micro-CT measurements and analyses. We also gratefully acknowledge Yehudit Hermesh, Ofira Higfa, and Neri Sharaby for expert animal care and Calanit Raanan for help with osteoclast histology preparations. This study was supported by the Israel Science Foundation (Grant 383/08), the Chief Scientist's Office of the Ministry of Health, Israel (Grant 3000005182), and the Kekst Family Institute for Medical Genetics and the David and Fella Shapell Family Center for Genetic Disorders Research, both of the Weizmann Institute.

REFERENCES

Amoui M, Sheng MH, Chen ST, Baylink DJ, Lau KH (2007). A transmembrane osteoclastic protein-tyrosine phosphatase regulates osteoclast activity in part by promoting osteoclast survival through c-Src-dependent activation of NFkappaB and JNK2. Arch Biochem Biophys 463, 47–59.

Andersen JN, Elson A, Lammers R, Romer J, Clausen JT, Moller KB, Moller NP (2001). Comparative study of protein tyrosine phosphatase-epsilon isoforms: membrane localization confers specificity in cellular signalling. Biochem J 354, 581–590.

Aoki K, Didomenico E, Sims NA, Mukhopadhyay K, Neff L, Houghton A, Amling M, Levy JB, Horne WC, Baron R (1999). The tyrosine phosphatase SHP-1 is a negative regulator of osteoclastogenesis and osteoclast resorbing activity: increased resorption and osteopenia in me(v)/me(v) mutant mice. Bone 25, 261–267.

Arias-Salgado EG, Lizano S, Sarkar S, Brugge JS, Ginsberg MH, Shattil SJ (2003). Src kinase activation by direct interaction with the integrin beta cytoplasmic domain. Proc Natl Acad Sci USA 100, 13298–13302.

Bauler TJ, Kamiya N, Lapinski PE, Langewisch E, Mishina Y, Wilkinson JE, Feng GS, King PD (2011). Development of severe skeletal defects in induced SHP-2-deficient adult mice: a model of skeletal malformation in humans with SHP-2 mutations. Dis Model Mech 4, 228–239.

Berman-Golan D, Elson A (2007). Neu-mediated phosphorylation of protein tyrosine phosphatase epsilon is critical for activation of Src in mammary tumor cells. Oncogene 26, 7028–7037.

Bodrikov V, Leshchyns'ka I, Sytnyk V, Overvoorde J, den Hertog J, Schachner M (2005). RPTPalpha is essential for NCAM-mediated p59fyn activation and neurite elongation. J Cell Biol 168, 127–139.

Boyle WJ, Simonet WS, Lacey DL (2003). Osteoclast differentiation and activation. Nature 423, 337–342.

Bruzzaniti A, Baron R (2006). Molecular regulation of osteoclast activity. Rev Endocr Metab Disord 7, 123–139.

Carlson J, Cui W, Zhang Q, Xu X, Mercan F, Bennett AM, Vignery A (2009). Role of MKP-1 in osteoclasts and bone homeostasis. Am J Pathol 175, 1564–1573.

Chellaiah MA, Kuppuswamy D, Lasky L, Linder S (2007). Phosphorylation of a Wiscott-Aldrich syndrome protein-associated signal complex is critical in osteoclast bone resorption. J Biol Chem 282, 10104–10116.

Chellaiah MA, Schaller MD (2009). Activation of Src kinase by protein-tyrosine phosphatase-PEST in osteoclasts: comparative analysis of the effects of bisphosphonate and protein-tyrosine phosphatase inhibitor on Src activation in vitro. J Cell Physiol 220, 382–393 .

Chen M, Chen SC, Pallen CJ (2006). Integrin-induced tyrosine phosphorylation of protein-tyrosine phosphatase-alpha is required for cytoskeletal reorganization and cell migration. J Biol Chem 281, 11972–11980.

Chiusaroli R, Knobler H, Luxenburg C, Sanjay A, Granot-Attas S, Tiran Z, Miyazaki T, Harmelin A, Baron R, Elson A (2004). Tyrosine phosphatase epsilon is a positive regulator of osteoclast function in vitro and in vivo. Mol Biol Cell 15, 234–244.

den Hertog J, Pals CE, Peppelenbosch MP, Tertoolen LG, de Laat SW, Kruijer W (1993). Receptor protein tyrosine phosphatase alpha activates pp60c-src and is involved in neuronal differentiation. EMBO J 12, 3789–3798.

Destaing O, Saltel F, Geminard JC, Jurdic P, Bard F (2003). Podosomes display actin turnover and dynamic self-organization in osteoclasts expressing actin-green fluorescent protein. Mol Biol Cell 14, 407–416.

Destaing O, Sanjay A, Itzstein C, Horne WC, Toomre D, De Camilli P, Baron R (2008). The tyrosine kinase activity of c-Src regulates actin dynamics and organization of podosomes in osteoclasts. Mol Biol Cell 19, 394–404.

Elefteriou F *et al.* (2005). Leptin regulation of bone resorption by the sympathetic nervous system and CART. Nature 434, 514–520.

Eleniste PP, Du L, Shivanna M, Bruzzaniti A (2012). Dynamin and PTP-PEST cooperatively regulate Pyk2 dephosphorylation in osteoclasts. Int J Biochem Cell Biol 44, 790–800.

Elson A, Leder P (1995a). Identification of a cytoplasmic, phorbol ester-inducible isoform of protein tyrosine phosphatase epsilon. Proc Natl Acad Sci USA 92, 12235–12239.

Elson A, Leder P (1995b). Protein-tyrosine phosphatase epsilon. An isoform specifically expressed in mouse mammary tumors initiated by v-Ha-ras OR neu. J Biol Chem 270, 26116–26122.

Gil-Henn H *et al.* (2007). Defective microtubule-dependent podosome organization in osteoclasts leads to increased bone density in Pyk2/mice. J Cell Biol 178, 1053–1064.

Gil-Henn H, Elson A (2003). Tyrosine phosphatase-epsilon activates Src and supports the transformed phenotype of Neu-induced mammary tumor cells. J Biol Chem 278, 15579–15586.

Gil-Henn H, Volohonsky G, Elson A (2001). Regulation of protein-tyrosine phosphatases alpha and epsilon by calpain-mediated proteolytic cleavage. J Biol Chem 276, 31772–31779.

Gil-Henn H, Volohonsky G, Toledano-Katchalski H, Gandre S, Elson A (2000). Generation of novel cytoplasmic forms of protein tyrosine phosphatase epsilon by proteolytic processing and translational control. Oncogene 19, 4375–4384.

Granot-Attas S, Luxenburg C, Finkelshtein E, Elson A (2009). PTP epsilon regulates integrin-mediated podosome stability in osteoclasts by activating Src. Mol Biol Cell 20, 4324–4334.

Jiang G, den Hertog J, Hunter T (2000). Receptor-like protein tyrosine phosphatase alpha homodimerizes on the cell surface. Mol Cell Biol 20, 5917–5929.
Jiang G, den Hertog J, Su J, Noel J, Sap J, Hunter T (1999). Dimerization inhibits the activity of receptor-like protein-tyrosine phosphatase-alpha. Nature 401, 606–610.
Kollet O *et al.* (2006). Osteoclasts degrade endosteal components and promote mobilization of hematopoietic progenitor cells. Nat Med 12, 657–664.
Kraut J, Volohonsky G, Toledano-Katchalski H, Elson A (2002). Nuclear localization of non-receptor protein tyrosine phosphatase epsilon is regulated by its unique N-terminal domain. Exp Cell Res 281, 182–189.
Krueger NX, Streuli M, Saito H (1990). Structural diversity and evolution of human receptor-like protein tyrosine phosphatases. EMBO J 9, 3241–3252.
Luxenburg C, Addadi L, Geiger B (2006a). The molecular dynamics of osteoclast adhesions. Eur J Cell Biol 85, 203–211.
Luxenburg C, Parsons JT, Addadi L, Geiger B (2006b). Involvement of the Src-cortactin pathway in podosome formation and turnover during polarization of cultured osteoclasts. J Cell Sci 119, 4878–4888.
Miyazaki T, Sanjay A, Neff L, Tanaka S, Horne WC, Baron R (2004). SRC kinase activity is essential for osteoclast function. J Biol Chem 279, 17660–17666.
Miyazaki T, Tanaka S, Sanjay A, Baron R (2006). The role of c-Src kinase in the regulation of osteoclast function. Mod Rheumatol 16, 68–74.
Nakamura K, Mizuno Y, Kikuchi K (1996). Molecular cloning of a novel cytoplasmic protein tyrosine phosphatase PTP epsilon. Biochem Biophys Res Commun 218, 726–732.
Peretz A, Gil-Henn H, Sobko A, Shinder V, Attali B, Elson A (2000). Hypomyelination and increased activity of voltage-gated K(+) channels in mice lacking protein tyrosine phosphatase epsilon. EMBO J 19, 4036–4045.
Ponniah S, Wang DZ, Lim KL, Pallen CJ (1999). Targeted disruption of the tyrosine phosphatase PTPalpha leads to constitutive downregulation of the kinases Src and Fyn. Curr Biol 9, 535–538.
Ross FP (2006). M-CSF, c-Fms, and signaling in osteoclasts and their precursors. Ann NY Acad Sci 1068, 110–116.
Rousso-Noori L, Knobler H, Levy-Apter E, Kuperman Y, Neufeld-Cohen A, Keshet Y, Akepati VR, Klinghoffer RA, Chen A, Elson A (2011). Protein tyrosine phosphatase epsilon affects body weight by downregulating leptin signaling in a phosphorylation-dependent manner. Cell Metab 13, 562–572.
Sartori R, Li F, Kirkwood KL (2009). MAP kinase phosphatase-1 protects against inflammatory bone loss. J Dental Res 88, 1125–1130.
Sheng MH, Amoui M, Stiffel V, Srivastava AK, Wergedal JE, Lau KH (2009). Targeted transgenic expression of an osteoclastic transmembrane protein-tyrosine phosphatase in cells of osteoclastic lineage increases bone resorption and bone loss in male young adult mice. J Biol Chem 284, 11531–11545.
Shivtiel S *et al.* (2008). CD45 regulates retention, motility, and numbers of hematopoietic progenitors, and affects osteoclast remodeling of metaphyseal trabecules. J Exp Med 205, 2381–2395.
Sines T, Granot-Attas S, Weisman-Welcher S, Elson A (2007). Association of tyrosine phosphatase epsilon with microtubules inhibits phosphatase activity and is regulated by the epidermal growth factor receptor. Mol Cell Biol 27, 7102–7112.
Soriano P, Montgomery C, Geske R, Bradley A (1991). Targeted disruption of the c-src proto-oncogene leads to osteopetrosis in mice. Cell 64, 693–702.
Su J, Muranjan M, Sap J (1999). Receptor protein tyrosine phosphatase alpha activates Src-family kinases and controls integrin-mediated responses in fibroblasts. Curr Biol 9, 505–511.
Takeda S, Elefteriou F, Levasseur R, Liu X, Zhao L, Parker KL, Armstrong D, Ducy P, Karsenty G (2002). Leptin regulates bone formation via the sympathetic nervous system. Cell 111, 305–317.
Tanuma N, Nakamura K, Kikuchi K (1999). Distinct promoters control transmembrane and cytosolic protein tyrosine phosphatase epsilon expression during macrophage differentiation. Eur J Biochem 259, 46–54.
Teitelbaum SL (2007). Osteoclasts: what do they do and how do they do it? Am J Pathol 170, 427–435.
Umeda S, Beamer WG, Takagi K, Naito M, Hayashi S, Yonemitsu H, Yi T, Shultz LD (1999). Deficiency of SHP-1 protein-tyrosine phosphatase activity results in heightened osteoclast function and decreased bone density. Am J Pathol 155, 223–233.
Wada T, Nakashima T, Hiroshi N, Penninger JM (2006). RANKL-RANK signaling in osteoclastogenesis and bone disease. Trends Mol Med 12, 17–25.
Yadav VK *et al.* (2009). A serotonin-dependent mechanism explains the leptin regulation of bone mass, appetite, and energy expenditure. Cell 138, 976–989.
Yang JH, Amoui M, Lau KH (2007). Targeted deletion of the osteoclast protein-tyrosine phosphatase (PTP-oc) promoter prevents RANKL-mediated osteoclastic differentiation of RAW264.7 cells. FEBS Lett 581, 2503–2508.
Zeng L, Si X, Yu WP, Le HT, Ng KP, Teng RM, Ryan K, Wang DZ, Ponniah S, Pallen CJ (2003). PTP alpha regulates integrin-stimulated FAK autophosphorylation and cytoskeletal rearrangement in cell spreading and migration. J Cell Biol 160, 137–146.
Zheng XM, Resnick RJ, Shalloway D (2000). A phosphotyrosine displacement mechanism for activation of Src by PTPalpha. EMBO J 19, 964–978.
Zheng XM, Wang Y, Pallen CJ (1992). Cell transformation and activation of pp60c-src by overexpression of a protein tyrosine phosphatase. Nature 359, 336–339.